

## MOS-like electroluminescent devices using silicon-rich oxide obtained by LPCVD

A. A. González Fernández, M. Aceves Mijares, Z. Yu, A. Morales Sánchez, K. M. Leyva  
INAOE, Luis Enrique Erro No. 1, Apdo. 51, Tonantzintla, Puebla 72000, México  
E-mail: agonzalez@inaoep.mx

**Abstract** — Silicon Rich Oxide (SRO) is a multiphase material composed by  $\text{SiO}_2$ , Si and  $\text{SiO}_x$ .(0<X<2). SRO characteristics include the photo and cathode emission of visible light. Lastly, big efforts have been devoted to obtain a controllable emission using electroluminescence, but keeping its compatibility with silicon IC's fabrication technology.

In this paper, electroluminescent properties of PolySi/SRO/Si structures were studied. Devices with two different Si excesses were characterized. A full area wideband emission is found on devices with the highest Si excess, the principal emitting bands are centered at 475 and 670 nm. The EL intensity of these bands is modulated by the applied electric field. Different emission colors were observed with the naked eye.

The 670 band present in devices with the highest Si excess is not found in those with the lowest Si excess. A discussion on the probable mechanism of emission is presented.

**Keywords** — Silicon rich oxide, electroluminescence (EL), dual-color emission, conductive paths.

### I. INTRODUCTION

As the integrated circuits (IC) industry demands higher integration levels and smaller dimensions, intra chip communication becomes a more serious problem and a bottleneck in the advances on this field. One approach to solve this problem is the change of the physical intra chip connections from metallic conductors to optical means. On the other hand, even when it is widely known that silicon (Si) dominates the microelectronics industry, bulk silicon has an indirect energy band gap and is therefore highly inefficient as light source. Then, much effort has been devoted to improve the Si light emission.

Since de observation of visible light emission from porous silicon at room temperature [1], Si nanostructures have received much attention due to the possibility of being used for opto electronic applications. One of these materials is Silicon Rich Oxide (SRO), which can be considered as a multi-phase material composed of a mixture of stoichiometric silicon oxide ( $\text{SiO}_2$ ), off-stoichiometric silicon oxide ( $\text{SiO}_x$ ,  $x < 2$ ) and elemental silicon (Si). After thermal annealing at high temperature, Si excess in SRO films agglomerates creating amorphous or crystalline Si nanoparticles [2]. There are several techniques to fabricate SRO films, including Implantation of Silicon into  $\text{SiO}_2$  (SITO) [3], Plasma Enhanced Chemical Vapor Deposition (PECVD) [4-6], and Low Pressure Chemical Vapour

Deposition (LPCVD) [4, 7]. The deposition technique that has shown the highest light emission intensity compared to others is LPCVD [3, 4]. In LPCVD, SRO is deposited using Silane ( $\text{SiH}_4$ ) and Nitrous Oxide ( $\text{N}_2\text{O}$ ) as reactive gasses and the excess silicon concentration is controlled varying the partial pressure ratio of the reactant gasses:

$$R_0 = \frac{P(\text{N}_2\text{O})}{P(\text{SiH}_4)}$$

Si excess as high as 17 at. % is obtained with  $R_0=3$ , and stoichiometric silicon oxide is obtained with  $R_0>100$  [5, 8, 9].

There have been some reports showing electro luminescence from Si-based devices [8-14]. However, almost no one shows naked eye visible EL in all the gate area, and very few uses LPCVD-SRO as active layer.

In this work, MOS-like functional electro luminescent devices with an LPCVD-SRO active layer were fabricated and studied.

### II. EXPERIMENTAL

Figure 1 shows a schematic of the fabricated devices. SRO layers were deposited using an LPCVD hot walls reactor at 720 °C. The substrates were *n*-type Si (100) wafers with a resistivity of 2-5 Ω-cm. SRO layers with different thicknesses and  $R_0$  values were used. Refractive index and thickness of the SRO layers were obtained with a Gaertner L117 ellipsometer on monitors. Table I lists the thickness and refractive indexes of SRO films.

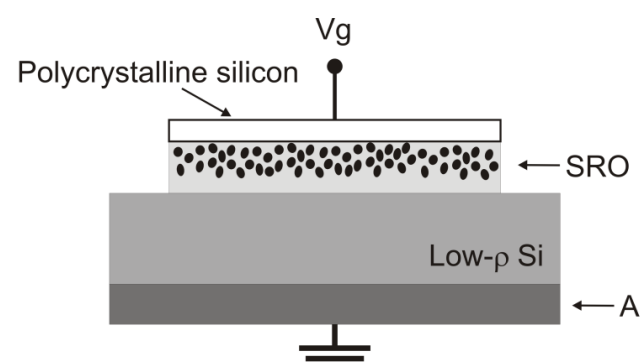


Fig. 1. Schematic representation of the electro luminescent devices fabricated.

TABLE I.  
 Characteristics of the fabricated SRO active layers.

Sample	$R_o$	SRO Thickness (nm)	Refractive index
1	30	$36.4 \pm 0.4$	1.48
2	30	$64.6 \pm 1.6$	1.54
3	30	$96.1 \pm 0.9$	1.55
4	45	$82.8 \pm 0.9$	1.47
5	45	$133.2 \pm 6.7$	1.47

All samples were submitted to a thermal annealing process at 1100 °C for 180 min in nitrogen atmosphere right after deposition. To use as semi-transparent gate, a heavily  $n$  doped polycrystalline silicon layer with thickness of  $t=300$  nm was deposited onto the SRO films. Lithography and etching processes were used to define a  $2 \times 2$  mm<sup>2</sup> square shaped gate. An aluminum layer of 1 μm of thickness was deposited in the back of the wafers and then annealed in forming gas.

Current–voltage (I–V) measurements were performed using a computer controlled Keithley 2400 source meter. Electrical stress was applied between the gate electrode and the back contact.

The EL spectra of fabricated devices were obtained using a HORIBA Jobin Yvon spectrofluorometer model Fluoromax-3 sweeping the detector monochromator from 350 to 950 nm with steps of 1 nm. Devices were biased with a constant DC voltage using a Keithley 2400 source meter.

In order to relate the current and the EL, I–V curves and EL properties were measured simultaneously. Voltage sweeps were programmed in the source meter and the current as a function of time was recorded. The emitted wavelengths readings were synchronized with the current through a computer’s program.

### III. RESULTS AND DISCUSSION

Two EL stages were observed in the fabricated devices. The first manifestation of EL in as-fabricated devices is as bright spots in the gate when a voltage is applied. This behavior has already been reported in previous works [15]. Figure 2 shows the EL spectra of the bright dots for both  $R_o=30$  and 45. The spectrum is similar for both  $R_o$ . They exhibit a broad band with a maximum peak at about ~625 nm.

The EL dots appear at both forward and reverse bias (accumulation and depletion of carriers in the substrate surface, respectively).

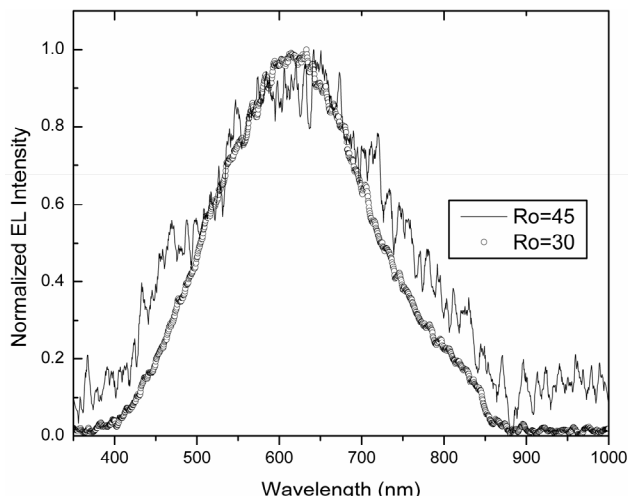


Fig. 2. Normalized EL spectra for bright dots in as-fabricated devices with active layer of  $Ro=30$  and 45, the thickness was 36.4nm and 83.6nm, respectively. The field applied was +2.5MV/cm in both cases.

In most cases, the luminescent spots are unstable and tend to disappear as the applied electric field increases. Figure 3 shows the typical I–V curves obtained for devices with  $Ro=30$  under forward bias ( $V_g > 0$ ). The curves obtained for as-fabricated devices (marked as “1st meas.”) present several current “jumps” and “drops”. This behavior is observed for different SRO thicknesses, as shown in figure 3. Bright spots are observed in this zone of current jumps and drops. However, when the electric field reaches a value between 3 and 4 MV/cm, the current drops abruptly and bright spots disappear. Current will not repeat the behavior of the first measurement in further tests.

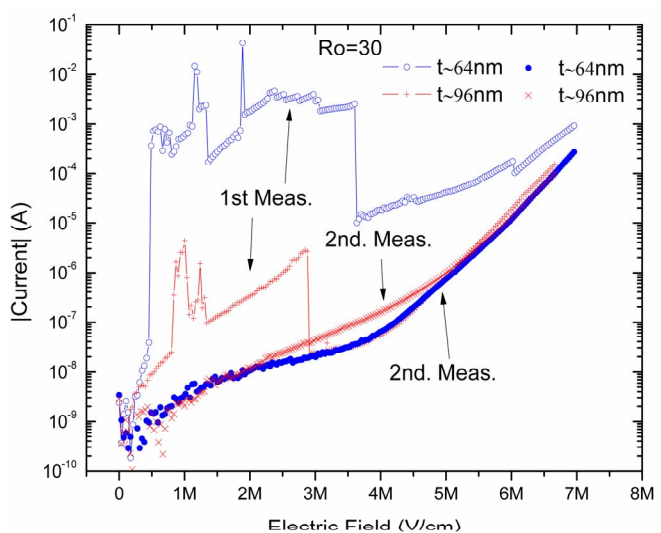


Fig. 3. Typical I–V curves in MOS-like devices with  $Ro=30$  under forward bias (accumulation). First measurement was done on as-fabricated devices, and the second measurement was done on the same device after 7 MV/cm were applied.

A subsequent I-V measurement (marked as “2nd meas”), on the same device, show a stable current at a low value for low electric fields, which is repeatable after the second measurement. No bright spots are observed after stabilization of the I-V curves. The switch between high and low conduction states due to the current jumps and drops has already been reported and it has been explained as the consequence of a complex mechanism of creation and annihilation of conductive paths [16].

The second EL stage is obtained only after the I-V curves are stabilized. It manifests as luminescence in the full area of the gate (FA-EL). Figure 4 presents pictures of this type of EL for devices with  $R_0=30$ . The FA-EL was observed in devices with both silicon excesses. The luminescence is visible with the naked eye as long as the applied electric field (EF) reach values of  $EF>4.5MV/cm$  for devices with  $R_0=30$  and  $EF>7MV/cm$  for devices with  $R_0=45$ .

It is important to remark that devices require the annihilation of the bright spots to present FA-EL; which is easily achieved by applying a voltage high enough to produce the current drop as shown in figure 3. According with the model presented in [16], before the annihilation of the conductive paths, the current does not flow uniformly through the whole device, but a high current conduction occurs in some discrete conductive paths, resulting in a higher amount of radiative recombination events in these discrete points [17]. Then the destruction of the preferential paths could permit the current to distribute in a more uniform way across the SRO volume, allowing the carriers to recombine radiatively in the full area.

The nature of the luminescence mechanism in SRO remains uncertain, but most works attribute it either to quantum confinement effects (QCE) [4, 8] or to several types of defects in the material surrounding Si nano-clusters [10, 13, 14, 18, 19].

Different emission intensities and colors were obtained in devices with  $R_0=30$  depending on the applied electric field, as can be seen in pictures of figure 4.

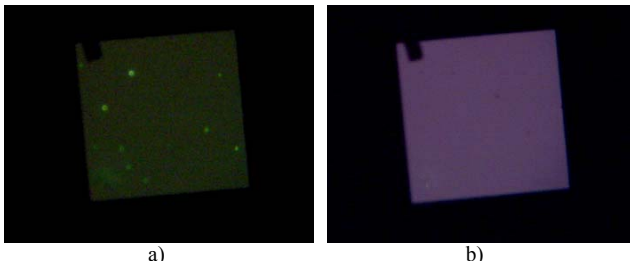


Fig. 4. Micro photography of an  $R_0=30$  device biased with a)  $EF=5$  MV/cm, and b)  $EF=7MV/cm$ . The EL is observed with the naked eye for both biases.

The spectra shown in figure 5a) clearly illustrates the two main emission bands. The peaks of these bands are located at  $\sim 475nm$  and  $\sim 680nm$  with no significant peak shifting with the applied electric field. The intensity of both EL peaks increases with voltage. This behavior was the same in all devices with  $R_0=30$  regardless the SRO thickness. The emission at  $\sim 475nm$  has been attributed to the presence of radiative defects in the active layer [14, 13], e.g. neutral oxygen vacancy defects (NOV), which have been found in SRO-LPCVD films with  $R_0=30$  [8]. The emission at  $680nm$  is usually attributed to QCE [6, 8, 14] but this is unlikely in this work given the absence of crystalline agglomerates reported in the material [2].

Figure 5b) shows the normalized EL to the highest emission of the two main EL bands. It can be observed how the  $680nm$  band has higher intensity than the  $475nm$  band under EF lower than  $\sim 6.5MV/cm$ . Beyond this value the higher energy emission ( $475nm$ ) is dominant, showing the blue-like light from the device observed in figure 4b). Therefore, the emission color can then be modulated with the applied electric field.

This dependence of the energy emission on applied electric field in the  $R_0=30$  devices is probably related to the carrier available energy. For electric fields  $<6.5$  MV/cm the majority of carriers can acquire only sufficient energy to excite the “red” ( $680nm$ ) emission states, while as the electric field applied increases more carriers gain sufficient energy to excite the “blue” ( $475nm$ ) emission [14].

As mentioned before, devices with  $R_0=45$  also present FA-EL. These devices did not show the dual-band spectra but a unique band centered in  $445nm$ , as shown in figure 6. Energy filtered transmission electron microscopy (EFTEM) studies performed on SRO films deposited under the same conditions that in this paper have shown no Si clusters in SRO with  $R_0$  values above 30 [2]. This could explain the absence of the red EL for  $R_0=45$ , being the formation of Si clusters during annealing the possible origin of the red emission in the  $R_0=30$  samples.

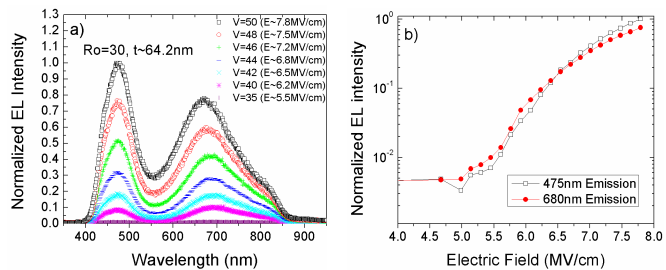


Fig. 5. a) EL spectra obtained from devices with  $R_0=30$  and  $t\sim 64.2nm$  emitting full area EL at different positive voltages. b) Normalized EL intensity at 475 and 680 nm as a function of the applied EF.

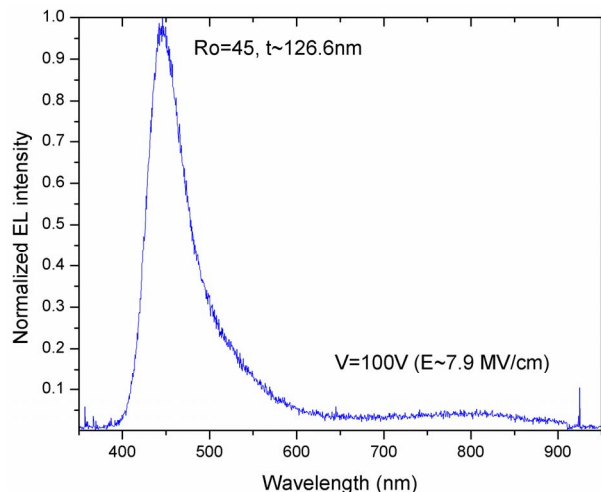


Fig. 6. EL spectra obtained from devices with  $R_o=45$ ,  $t\approx 126.6\text{nm}$  emitting full area EL applying +100V in the gate.

The EL in these SRO-based devices has proved to be very complex, and a detailed and intensive study is in process to better understand our results.

### III. CONCLUSION

Silicon based light emitting devices fully compatible with CMOS technology were fabricated. Two EL stages are observed.

The first EL stage is manifested as shining spots in as-fabricated devices and for positive electric fields below  $4\text{MV}/\text{cm}$  and  $E_F=7\text{MV}/\text{cm}$  for devices with  $R_o=30$  and  $R_o=45$ , respectively. This first EL phase corresponds to a stage of “current jumps” in the I-V curves of the devices, which could exist due to the creation and annihilation of preferential conduction paths; these may also be related to the appearing and disappearing of shining spots.

The second EL stage is shown only after the current stabilization and for electric field values higher than  $4.5\text{MV}/\text{cm}$  and  $7\text{MV}/\text{cm}$  for devices with  $R_o=30$  and  $R_o=45$ , respectively. The luminescence manifests evenly in all the gate area. The disappearing of all bright spots is related with the annihilation of preferential conductive paths that may be responsible for an uneven distribution of current, achieved by the application of an electrical treatment.

The emission wavelength of the shining spots was the same for both  $R_o$ , while the full area emission spectra characteristics depend on the Si concentration in the active SRO layer. However, they both show a wide spectrum. For  $R_o=30$ , two principal emission bands were observed at 475 and 680nm. Moreover, the dominating color emission was

modulated by the applied electric field. For samples with  $R_o=45$  a single dominating emission band at 445nm was observed.

### ACKNOWLEDGMENT

The authors acknowledge the support received from Consejo Nacional de Ciencia y Tecnología (CONACyT). The authors also thank Pablo Alarcón, Manuel Escobar, Mauro Landa, Netzahualcoyotl Carlos and Ignacio Juárez for their help in preparing the samples and characterization.

### REFERENCES

- [1]. L.T. Canham, “Visible light emission due to quantum size effects in highly porous crystalline silicon”, *Appl. Phys. Lett.* 57 (1990) 1046.
- [2]. J. A. Luna-López, A. Morales, M. Aceves, C. Domínguez, "Analysis of surface roughness and its relationship with photoluminescence properties of silicon-rich oxide films", *J. Vac. Sci. Technol. A27*, pp. 57-62, 2009.
- [3]. F. Flores Gracia, M. Aceves, J. Carrillo, C. Domínguez, C. Falcony, “Photoluminescence and cathodoluminescence characteristics of SiO<sub>2</sub> and SRO films implanted with Si”, *Superficies y Vacío* 18(2), 7-13, Junio de 2005, pp 7-13.
- [4]. A. Morales, J. Barreto, C. Domínguez, M. Riera, M. Aceves, J. Carrillo, "Comparative study between silicon-rich oxide films obtained by LPCVD and PECVD", *Physica E: Low-dimensional Systems and Nanostructures*, Vol 38, April 2007, pp. 54-58.
- [5]. F. Iacona, G. Franzò, and C. Spinella, “Correlation between luminescence and structural properties of Si nanocrystals”. *J. Appl. Phys.* 87 (3) (1999).
- [6]. G. Franzò, A. Irrea, E. C. Moreira, M. Miritello, F. Iacona, D. Sanfilippo, G. Di Stefano, P.G. Fallica, F. Pirolo, "Electroluminescence of silicon nanocrystals in MOS structures". *Appl. Phys.* 74 (2001).
- [7]. Nicolas Buffet, Pierre Mur, Barbara De Salvo, Marie Noelle Semeria, “Silicon nano-crystals precipitation in a SiO<sub>2</sub> matrix elaborated from the decomposition of LPCVD SiO<sub>x</sub>”, *IEEE Nano 2002* pp. 269-272.
- [8]. D. J. DiMaria, J. R. Kirtley, J. Pakulis, D. W. Dong, D. Kuan , F. L. Pesavento, T. N. Theis, N. Cutro, S. D. Brorson, “Electroluminescence studies in silicon dioxide films containing tiny silicon islands”, *J. Appl. Phys.* Vol. 56, No 2, p. 401-416, (1984).
- [9]. M. Aceves, C. Falcony, A. Reynoso, W. Calleja, A. Torres. “The conduction properties of the silicon

- /off-Stoichiometric SiO<sub>2</sub> diode" *Solid-State Electronics* 39, 637 (1996).
- [10]. Ding, L.; Chen, T. P.; Liu, Y.; Wong, J. I.; Liu, K. Y, "The influence of the implantation dose and energy on the electroluminescence of Si<sup>+</sup> implanted amorphous SiO<sub>2</sub> thin films", *Nanotechnology* 18 (2007)
- [11]. Irrea, Alessia, Iacona, Fabio and Crupi, Isodiana, "Electroluminiscence and transport properties in amorphous silicon nanostructures", *Nanotechnology* 17 (2006). pp. 1428-1436.
- [12]. O. Jambois, H. Rinnert, X. Devaux, M. Vergnat, "Photoluminescence and electroluminescence of size-controlled silicon nanocrystallites embedded in SiO<sub>2</sub> thin films", *J. Appl. Phys.* 98 (2005) 046105-1–046105-3.
- [13]. Gong-Ru Lin, Chun-Jung Lin, "Improved blue-green electroluminescence Si-implanted and annealed SiO<sub>2</sub>/Si substrate", *J. Appl. Phys.* 95 (12) (2004) 8484–8486.
- [14]. W. K. Tan, Q. Chen, J. D. Ye, M. B. Yu, Guo-Qiang Lo, D.-L. Kwong, "Dual-Color Electroluminescence (λ~450nm and 650-700nm) From a Silicon-Based Light Source" *IEEE Electron. Dev. Lett.* 29 (2008).
- [15]. A. Morales. Correlation between optical and electrical properties of materials containing nanoparticles. PhD. Thesis, Universitat Autònoma de Barcelona, 2008.
- [16]. A. Morales-Sánchez, J. Barreto, C. Domínguez, M. Aceves and J. A. Luna-López, "The mechanism of electrical annihilation of conductive paths and charge trapping in silicon-rich oxides", *Nanotecnology* 20 (2009).
- [17]. A. Morales-Sánchez, J. Barreto, C. Domínguez, M. Aceves, J. A. Luna-López, M. Perálvarez, B. Garrido, "Alternating electroluminescence mechanisms in silicon-rich oxide films", *Nanotecnology*, in press.
- [18]. Sopinsky M., Khomchenko V., "Electroluminescence in SiO<sub>x</sub> films and SiO<sub>x</sub>-film-based systems", *C. O. Sol. State and Mat. Sci.* 7, (2003) .
- [19]. Chun-Jun Lin, Gong-Ru Lin, "Defect-Enhanced Visible Electroluminescence of Multi-Energy Silicon-Implanted Silicon Dioxide Film", *IEEE Jour. Quant. Elec.* 41 (2005).